

ELECTRON-CLOUD DYNAMICS IN HIGH-INTENSITY RINGS*

L. Wang and J. Wei, BNL, Upton, NY 11973, USA

Abstract

Electron cloud is one of the main limitations in high-intensity rings. Electrons generated and accumulated inside the beam's pipe form an "electron cloud" that interacts with the circulating charged-particle beam. With a sizeable number of electrons, these interactions can cause instability, loss of the beam, and the growth of emittance. At the same time, the vacuum pressure will rise due to the desorption of electrons. This presentation gives an overview of the mechanism and dynamics of typical electron multipacting in various magnetic fields, and suggests mitigation measures for different beams.

INTRODUCTION

Electron cloud due to multipacting can cause transverse beam instabilities, beam loss, vacuum pressure rise and transverse beam size increase. Multipacting is induced by beam itself [1]. Electrons gain energy from the beam. The energy gain is proportional to the square root of the beam line density for a long bunch. It is proportional to the beam line density for an intermediate bunch. Therefore, multipacting happens in high intensity rings where electrons can gain sufficient energy for multipacting. The electron cloud have been observed in almost all the recent intensity rings, such as LANL PSR, KEKB, PEP-II, AGS, SPS. The mechanism of, and phenomena involved in multipacting vary with the beam's parameters, such as the bunches' spacing, intensity, length, shape, and so on. They also vary with the aperture of beam's pipe and the electric-magnetic field inside the chamber. This paper briefly describes the phenomena and mechanism of electron multipacting in different beam and fields.

MECHANISMS OF MULTIPACTING FOR DIFFERENT BEAMS

Three kinds of typical multipacting are addressed in the following paragraphs according to the transit number n , which is the number of electrons crossing the vacuum pipe during the passage of one bunch. Table 1 lists the typical parameters used in this paper.

Trailing Edge Multipacting with a Long Bunch ($n \gg 1$, SNS Case)

All electrons remaining inside the chamber before the approaching bunch (those surviving from the last bunch gap) along with electrons generated by ionisation can be trapped inside the beam during a bunch's passage and

released at its end. They are dynamically important, causing beam instability because huge numbers of them can be deeply trapped inside it. They have a weak effect on multipacting due to their long-term trapping and low energy at the chamber's surface.

Electrons born at the wall between the bunches' center and tail are the only source of multipacting due to their making multiple hits on the wall, and gaining sufficient energy when they hit the chamber's surface at the bunch's tail. The energy gain from the beam when it hits the chamber surface is sensitive to its longitudinal profile [2]

$$\Delta E = -f(a, b) \frac{\partial \lambda}{\partial z} \frac{1}{\sqrt{\lambda}} \quad (1)$$

where f is a function of beam's size, a , and the aperture of beam's pipe, b . λ is the longitudinal profile of the beam. From Eq. (1), there is a big energy gain at the bunch's tail (FIG. 1) that explains the mechanism of multipacting at the trailing edge [3-4]. A coasting beam has zero energy gain, and hence, there is no multipacting. The peak energy gain in both the SNS and PSR beams is less than 400 eV. A small pipe aperture results in a low energy gain [2]. Therefore, electron multipacting can be suppressed by choosing a pipe with a small aperture [5].

Table 1: Basic parameters of the KEKB LER, RHIC, and the SNS rings

Variable	KEKB	RHIC	SNS
beam size a (mm)	0.42/0.06	2.4	28
Chamber radius b (mm)	50	35~60	100
Bunch length (ns)	0.05	5~35	700
Beam intensity $N(\times 10^{10})$	3.3	10	20000
Bunch spacing (ns)	8/2	216	200
Transit number n	$\ll 1$	~ 1	~ 70

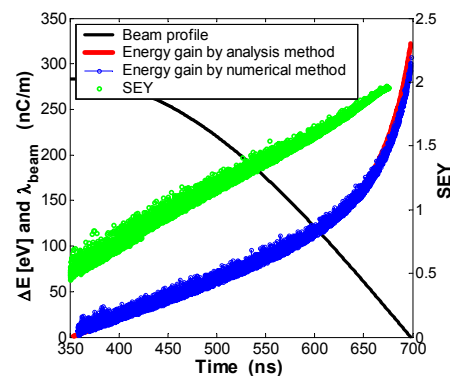


Figure 1: Energy gain and secondary emission yield (SEY) of multipacting electrons in the drift region of the SNS ring. The energy gain is high at the bunch tail.

*Work performed under the auspices of the U.S. Department of Energy. The SNS is managed by UT-Battelle, LLC, under contract DE-AC05-00OR22725 for the U.S. Department of Energy. It is a partnership of six national laboratories: Argonne, Brookhaven, Jefferson, Lawrence Berkeley, Los Alamos, and Oak Ridge.

Intermediate Bunch Length With Long Bunch Spacing—the Energy Gain Depends On a Single Bunch's Line Density and an Electron's Radial Coordinate, Alternate Multipacing ($n \sim 1$, RHIC)

In the RHIC, an electron typically hits the surface of the beam's chamber once during the passage of the bunch. Multipacting may occur if the electron's level of energy is suitable when the beam sweeps it to the chamber's surface. It may survive during the passage of the bunch gap by being reflected several times due to its low energy. The positive ions inside chamber also help the electron's survival by reducing the effect of its space charge.

When an electron cloud encounters the sequential bunches, its transverse distribution is close to uniform due to diffusion during the bunch gap; it typically has an energy of a few eV . The energy gain of an electron from the incoming bunch strongly depends on its transverse position when it meets the bunch [6, 7], but also is weakly dependent on its own velocity. Fig. 2 shows the energy gain as a function of the electron's radial coordinate when it meets the approaching bunch. The peak gain in energy is proportional to the beam's line density

$$\Delta \hat{E} = 70 \bar{\lambda} (eV) = 70 e Z N / \sigma (eV) \quad (2)$$

where $\bar{\lambda}$ is the beam line density in C/s , e is the electron charge, N is the bunch intensity, Z the charge number per particle ion, and σ is the bunch's length in seconds. The radial coordinate at peak energy gain increases with the bunch's length. The energy gain has more small peaks near the chamber's center where an electron executes more oscillations during the bunch's passage than at the chamber's edges. The peak energy gain in RHIC is about 500 eV . Unlike the case of the long bunch (Eq.1), in RHIC the energy gain is not directly related to the aperture of the beam's chamber, although the integrated energy spectrum is. Multipacting in RHIC can be suppressed by reducing the beam line's density (by reducing the bunch's intensity or increasing its length) or by having a pipe with a small aperture because the energy gain is small with a small radial coordinate. For example, there is no multipacting with a bunch length of 15ns and a pipe aperture of 20mm but it does occur when the aperture is 36mm. A pressure rise was observed at RHIC during beam rebucketing due to bunch shortening [8].

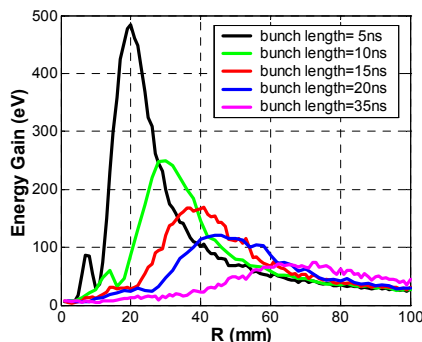


Figure 2: The electron's average gain in energy as a function of its initial position when it meets the following bunches. Proton bunch intensity, N , is 1×10^{11} .

Short Bunch with Short Spacing—the Energy Gain Depends on Multibunch, Random Multipacting ($n \ll 1$, B-Factories)

In the KEKB and PEP-II, an electron receives multiple bunch kicks from the beam before it hits the wall. Typically, it takes 2~3/5~6 bunch spacing for an electron to cross the chamber in the KEKB with the parameters shown in Table 1.

Simulation shows that the integrated energy spectrum of electrons inside the chamber is continuously and monotonously distributed. However, there are many structures within that of the electrons hitting the wall [9]. The spectrum at some energy ranges is very low, similar to the "stop-band" in wave transmission. We also use this term for this kind of structure in the energy spectrum. E-CLOUD revealed a similar phenomenon [10]. The structure in the energy spectrum of electrons that hit the wall reflects the multibunch effect. Fig. 3 is a snapshot of the electrons' distribution inside the chamber plotted as a function of energy and radial coordinate. It clearly reveals the dependence of the energy distribution on radial position. The "stop-band" in the spectrum of electron at the wall is derived from that of the electrons inside the chamber. The discreteness in the energy spectrum is a major characteristic of the electron cloud in a short bunch machine. It reflects the effect of multiple passages of the positron/proton bunches. The number of "stop-bands" depends only on the beam (the bunches' spacing and intensity) and the radius of the beam's chamber. It corresponds to the length of time in bunch spacing during which electrons can transit the chamber. For example, as shown in Fig. 3, it takes at least 5~6 bunch spacing for electrons to transit the chamber. The structure of energy spectrum is sensitive to the bunches' spacing and current, and the chamber's size. There are more structures in the energy spectrum when the spacing or the chamber's aperture is small because then more bunches will kick the electrons during their movement from the wall to the opposite surface. For the same reason, there also is more structure in the spectrum with a low beam intensity. The energy gain has a wide spread, up to keV .

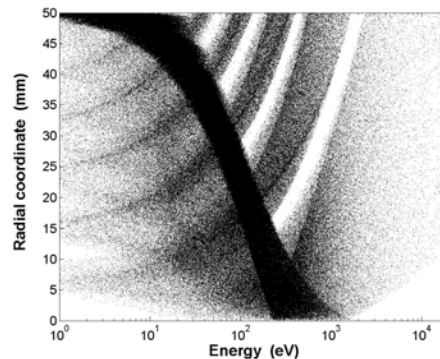


Figure 3: Snapshot of the electrons' distribution as a function of energy and radial coordinate with 2 ns bunch spacing.

MUTIPACTING IN A DIPOLE MAGNET

FIG. 4 shows the simulated distribution of an electron cloud inside a dipole magnet of the KEKB LER. Multipacting strips are clearly visible in the figures. The CERN SPS experiments exhibited similar multipacting strips in a dipole magnet [11]. The energy gain has peak at the horizontal center and decreases with the horizontal coordinate [12]. For a beam with low intensity, multipacting occurs at the horizontal center where the energy gain is typically a few hundreds eV , and hence, the secondary emission yield (SEY) is bigger than 1. With a high intensity beam, the energy gain at the horizontal center is more than thousands eV and exceeds the value at which SEY is bigger than 1. It is well known that the true SEY is smaller than 1 for electrons with both very high and very low energy. Consequently, multipacting occurs in two regions on either side of the horizontal chamber's center. The position of the multipacting region depends on the energy of the electrons, which is determined by the interactions of electrons and bunches. Therefore, the filling pattern of the beam, including bunch current and spacing, can alter the regions with strong multipacting. In general, when the bunch current increases, the multipacting region moves towards larger $|x|$ on either side of the center.

In the dipole magnets of SNS ring, the peak energy gain at horizontal center typically is less than $350eV$ [2]. Therefore, only electrons moving near the center of the horizontal chamber have enough energy at the wall's surface to form a multipacting cloud. As a result, there is only one strip of electron cloud at chamber's horizontal center in the present-day long-bunch machines (FIG. 5). The energy gain in a strong dipole magnet has the same dependence on the beam's longitudinal profile as that in a drift region. Therefore, there is a similar pattern of build-up and multipacting at the bunch's tail. The difference in the motion of electron cloud is that it is trapped vertically by the beam's space-charge force at the chamber's center during the beam's passage.

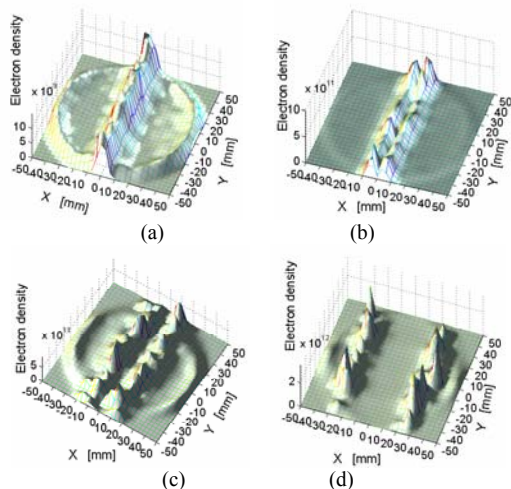


Figure 4: Strips of an electron cloud in a dipole field of KEKB LER at different bunch intensities: 1.1×10^{10} (a), 3.3×10^{10} (b), 9.9×10^{10} (c), 2.0×10^{11} (d).

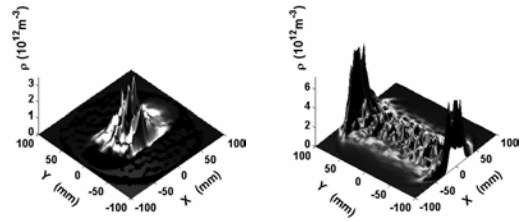


Figure 5: Electrons' transverse distribution in the SNS dipole magnet at bunch's center (left) and tail (right).

TRANSVERSE TRAPPING AND LONGITUDINAL SWEEPING IN QUADRUPOLE MAGNET

In short-bunch rings, such as the KEKB LER, the photoelectrons can be transversely trapped inside a quadrupole- and sextupole-magnet due to mirror-field trapping (FIG. 6)[13,14]. They move slowly in the beams' longitudinal direction due to $\mathbf{E} \times \mathbf{B}$ drift, centrifugal force drift, and magnetic gradient drift. This trapping is induced by beam and it is sensitive to the bunches' length and spacing [13]. A short bunch effectively increases the electrons' energy of gyration and so traps them.

In a quadrupole magnet of the SNS ring, the beam's space-charge transversely confines the electron cloud to the chamber's center and the four mirror-field regions, so minimizing the transverse size of the electron cloud at the bunch's center. The electrons are released at the tail and multipacting occurs near the middle regions of the magnetic pole (FIG. 7a).

With an intense beam like the SNS, the effect of $\mathbf{E} \times \mathbf{B}$ drift is important in a quadrupole magnet due to the strong beam's space-charge field and the weak magnetic field:

$$\mathbf{v}_{EB} = \frac{\mathbf{E} \times \mathbf{B}}{B^2} \quad (3)$$

The $\mathbf{E} \times \mathbf{B}$ drift in the longitudinal direction, which depends on the transverse position of the electrons. Half of them move in the beam's direction while the other half move in the reverse direction. Therefore, a quadrupole magnet with a high-intensity beam can effectively transport electrons longitudinally. Accordingly, electrons are swept out of the quadrupole. As a result, fewer electrons can accumulate inside a short quadrupole magnet (FIG. 7b).

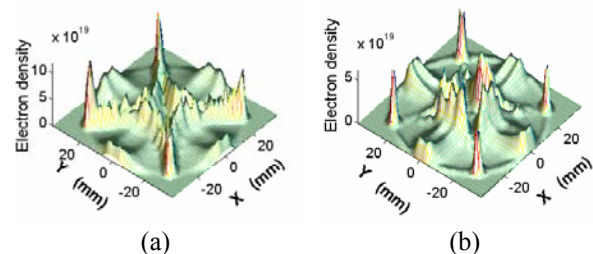


Figure 6: Distribution of the electron cloud in SUPERKEKB during the bunch's passage (a), and at

bunch's gap (b). The bunch intensity is 5.2×10^{11} and its spacing is 2 ns.

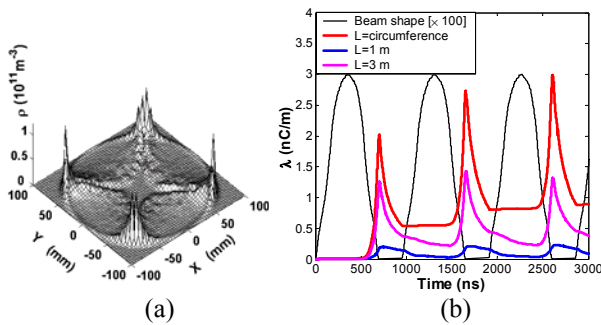


Figure 7: Distribution at the bunch tail (a) and build-up (b) of electron cloud in the SNS's quadrupole magnet. The effect of $\mathbf{E} \times \mathbf{B}$ drift is shown in (b) for different lengths, L , of the magnet.

REMEDIES

Solenoid

A solenoid satisfactorily suppresses multipacting in the drift region by confining the electrons close to the walls' surface. The required strength of the solenoid field can be estimated using the criterion

$$\rho \ll a \quad (4)$$

where ρ is the radius of the electron's orbit

$$m_e v^2 / \rho = e(vB - E) \quad (5)$$

where E is the beam's space-charge field, B is the solenoid field, and m_e and e are the mass and charge of the electron, respectively. For the SNS, a weak solenoid of 30 Gauss can confine the electrons near the wall and totally suppress multipacting, thereby reducing the electron's energy. The required field for KEKB is 50 Gauss. FIG. 8 shows the effects of a solenoid on an electron cloud in the SNS ring.

When the bunch gap is longer than the half period of the electron's gyration, the threshold of multipacting depends only on the beam's intensity. However, when the gap is shorter, it also depends on the bunch's spacing and the solenoid field. Reflection electrons with low energy induce the resonance phenomenon of electron cloud build-up at certain fields [15~17]. As shown in Eqs (4-5), the required field is a function of beam's intensity (space-charge field): a stronger solenoid field is needed for a high intensity beam as demonstrated in the simulation depicted in FIG. 9.

Fig. 10 shows the wake field with 10 G and 20 G uniform solenoid fields in the KEKB LER. Two frequency components appear, as shown by the FFT of the wake. One depends on the electron cloud's space charge; therefore, it is modulated by both the distribution and density of electron cloud, and its frequency usually decreases with increasing strength of the solenoid fields. It is similar to the traditional bounce frequency, which ranges from a few MHz to 50 MHz in the KEKB machine. The other frequency component (the fast one in Fig 9) comes from the gyration of the electrons [15]. For

example, the cyclotron's frequency is about 29MHz in a 10G field.

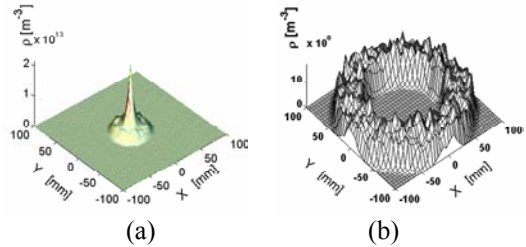


Figure 8: Electron cloud's transverse distribution in a 0-Gauss (a) and 30-Gauss (b) solenoid field during passage through the bunch center in the SNS ring.

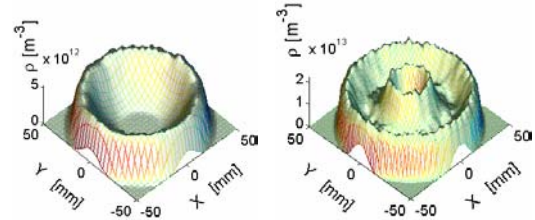


Figure 9: Electron distribution with a 10G solenoid field and bunch intensity $4/8 \times 10^{10}$ (left/right) in the KEKB LER.

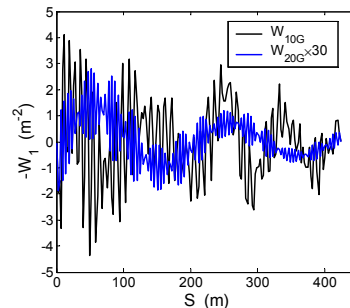


Figure 10: Long-range wake fields of the electron cloud with a 10-Gauss solenoid field in the KEKB LER. We note that the wake with the 20G field is enlarged 30 times to make it visible. The bunch spacing is 8 ns.

Clearing electrodes

A weak solenoid magnetic field does not work in magnets, where serious multipacting and trapping can occur. A low potential barrier near the chamber can capture photoelectrons both in the drift region and inside the magnets with very good clearing effects [18]. This kind of potential can be generated by clearing electrodes consisting of negatively charged strip lines paralleling the vacuum chamber, so that the electric field they provide can repel the electrons and reflect them back to the chamber's walls. FIG. 11 shows the potential of one group of electrodes consisting of 4 and 2 strip lines. Such electrodes generate a strong trapping field around the chamber's walls, while the clearing field at the center region of the vacuum is close to zero. This configuration (a) can be used in both the drift region and quadrupole magnet, and (b) for a dipole magnet. The required voltage is -200V and -400V , respectively, in the drift region and dipole magnet of KEKB LER.

A clearing system was applied to the SNS injection area and the Beam Position Monitors (BPMs) were modified as clearing electrodes. In principle, to suppress the electron cloud, the strength of a clearing field must be equal to the beam's space-charge field at the wall's surface to restrain the emission of secondary electrons. In the drift region of the SNS ring, this required field is 5,000 volts. However, a low clearing voltage of 200 Volts proved efficient, while an intermediate voltage of 2,000 volts may introduce strong multipacting [19]. This phenomenon happens only in long-bunch rings.

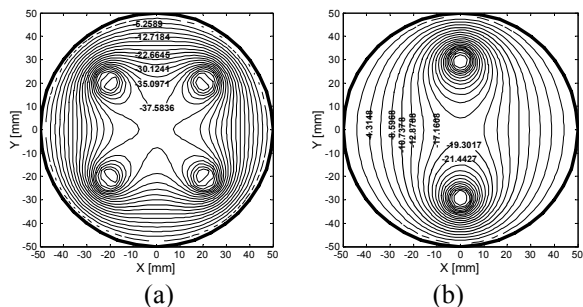


Figure 11: The potential barrier of the clearing field for different configurations with a clearing voltage of $-100V$ (a), and $-200V$ (b)

Collection of stripped electron

FIG. 12 illustrates the mechanism of collecting stripped electrons at the SNS's Accumulator Ring. To control their movement, the foil is placed in a magnetic field, which is part of the injection bump. The stripped electrons are guided by the magnetic field and collected by an electron catcher located at the bottom of the chamber. To ensure that the stripped electrons are not reflected upward before reaching the electron catcher, the low pole surface of the magnet is extended downstream by about 20 cm.

The catcher has a serrated shape with slightly overhanging surface so that electrons can be confined inside and hit the catcher's surface a several times before they die out or are reflected. Electron collection is sensitive to catcher's geometry, position, and material. The good catcher zone has width of 10 mm and 15 mm in vertical and longitudinal direction, respectively. A carbon catcher was chosen for the SNS considering its small backscattered electron yield. Simulation shows this catcher can retain 99.6% of the stripped electrons. FIG. 13 shows the distributions of the stripped electron cloud at the SNS injection region [5, 20].

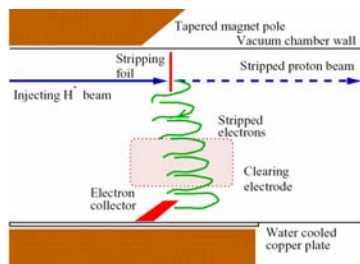


Figure 12: Collection of stripped electrons during the injection of the H-beam at the SNS ring.

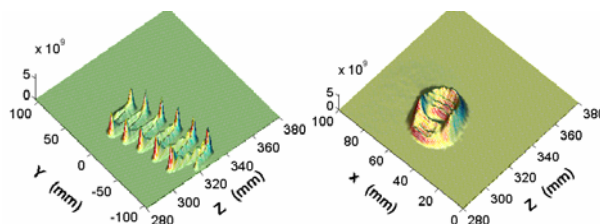


Figure 13: Distributions of the electron cloud with a carbon catcher in different planes.

E-CLOUD WITH TWO-BEAMS

The rise in vacuum pressure at the interaction region of RHIC limits the beam's intensity because of its double current and short bunch spacing there, and hence, there is a low threshold for multipacting. The beam's pattern, and hence, multipacting is a function of the longitudinal position z . FIG. 14 shows the simulated longitudinal distribution of electrons during one bunch spacing period. The origin of z is the interaction point (IP). There is no electron cloud near the IP because of the high energy-gain there [8]. The width of the electron-free zone increases with the bunch's intensity.

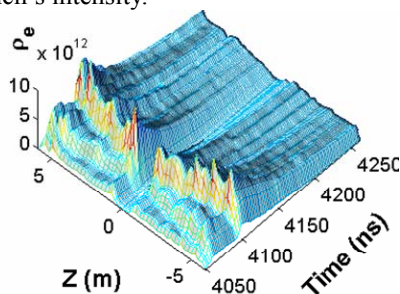


Figure 14: Distribution of the E-cloud with two beams in an interaction region of RHIC.

REFERENCES

- [1] Gröbner, PAC77, p. 277; also PAC97, p. 3589.
- [2] L. Wang, *et al*, Phys. Rev. E, V70, 036501(2004)
- [3] R. Macek, PSR Technical Note, PSR-00-10
- [4] V. Danilov, *et al*, AIP Conf. Proc. No. 496, p. 315.
- [5] L. Wang, *et al*, these proceedings, FPAP024.
- [6] S. Berg, LHC Project Note 97, CERN, 1997.
- [7] S. Heifets, CERN-2002-001, p.129
- [8] G. Rumolo and W. Fisher, BNL Note C-A/AP/146
- [9] L. Wang, A. Chao, H. Fukuma, CERN-2005-001
- [10] F. Zimmermann, CERN-2002-001.
- [11] J.M. Jimenez, *et al*, CERN-2002-001, 2002
- [12] L. Wang, *et al*, Phys. Rev. ST-AB, V5, 124402 (2002)
- [13] L. Wang, *et al*, Phys. Rev. E, V66, 036502 (2002)
- [14] G. Rumolo and F. Zimmermann, CERN-2002-001, p97
- [15] L. Wang, *et al*, CERN-2005-001
- [16] A. Novokhatski, J. Seeman, SLAC-PUB-9950
- [17] Y. Cai, M. Pivi, M. Furman, Phys. Rev. ST-AB 7, 024402, 2004
- [18] L. Wang, H. Fukuma and S. Kurokawa, KEK Preprint 2003-137
- [19] L. Wang, *et al*, Phys. Rev. ST-AB, V7, p34401, 2004
- [20] Y.Y. Lee, *et al*, these proceedings, WPAE035.